micro

MDPI

Article

Preparation and Characterization of a Ni/Cu–Phosphinate Material with Methylene Blue Removal Properties

Diana Anghel *, Gheorghe Ilia, Vlad Chiriac and Dana Vlascici *

Department of Chemistry, Faculty of Chemistry, Biology, Geography, West University Timisoara, 16 Pestalozzi Street, 300115 Timisoara, Romania; gheorghe.ilia@e-uvt.ro (G.I.); vlad.chiriac@e-uvt.ro (V.C.)
* Correspondence: diana.anghel@e-uvt.ro (D.A.); dana.vlascici@e-uvt.ro (D.V.)

Abstract

A Ni/Cu-containing phosphinate material based on 2-carboxyethyl(phenyl)phosphinic acid was synthesized under hydrothermal conditions and characterized using FT-IR (Fourier Transform Infrared Spectroscopy), SEM (Scanning Electron Microscopy) and EDAX (Energy Dispersive X-ray Analysis) analysis. The FT-IR spectra suggest the coordination of the phosphinate group to the metal, while SEM revealed compact aggregated particles of the compound. EDAX analysis confirmed the simultaneous presence of both Ni(II) and Cu(II) metals in the synthesized material. DFT (Density Functional Theory) calculations performed on the corresponding mononuclear Ni-CEPPA and Cu-CEPPA models indicated that the Cu complex possesses a smaller HOMO–LUMO energy gap (2.72 eV) than the Ni analog (3.43 eV), suggesting higher electronic reactivity. The obtained material was preliminarily evaluated for Methylene Blue removal, exhibiting an adsorption capacity of 170.24 mg/g. These results suggest that mixed Ni/Cu phosphinate materials may represent potential candidates for adsorption-related applications.

Keywords: phosphinate ligand; mixed-metal system; methylene blue adsorption

1. Introduction

In the past few years, complexes based on Ni(II) [1] and Cu(II) [2] ions have been intensively studied due to their diverse coordination modes, distinct electronic configurations and potential sensing and adsorption applications. These metal ions form stable complexes with ligands that contain donor oxygen atoms [3].

Phosphinate ligands attract considerable attention due to their strong affinity toward metal centers and the ability to form different coordination modes: mono-, bi- or polydentate [4,5]. Considering all those characteristics, as well as the presence of phosphorous-containing functional groups, the resulting compounds are suitable for various technological applications [6].

The 2-carboxyethyl(phenyl)phosphinic acid is of particular interest due to the presence of phosphinate and carboxylate groups, providing multiple coordination sites.

Studies regarding mixed Ni(II)/Cu(II) systems based on phosphinates are limited, especially regarding their structural and morphological properties.

The combination of transitional metals (such as Ni(II) and Cu(II)) with ligands like CEPPA can lead to the formation of mixed-metal systems with interesting morphological and structural proprieties. It also may provide enhanced electronic and adsorption properties due to the coexistence of different metal-centered electronic environments [2].

Check for updates

Academic Editors: Constantinos Salmas, Michalis Karakassides and Nikolaos Chalmpes

Received: 15 June 2026
Revised: 31 July 2026
Accepted: 6 August 2026
Published: 19 August 2026

Copyright: © 2026 by the authors. Licensee MDPI, Basel, Switzerland. This article is an open access article distributed under the terms and conditions of the Creative Commons Attribution (CC BY) license.

Computational studies such as DFT and TD-DFT calculations are employed to investigate the electronic structures and optical properties of the metals involved in this study.

Recent studies showed that bimetallic systems frequently exhibit enhanced adsorption behavior compared to monometallic analogs due to cooperative metal–ligand interactions and modified surface/electronic properties [7,8].

Methylene Blue (MB) is a cationic phenothiazine dye that is widely used as a model pollutant in adsorption investigations due to its strong visible absorption, high aqueous stability, and facile UV–Vis detection [9]. The increasing environmental concerns associated with dye-containing industrial effluents have stimulated the development of novel adsorption materials for MB removal from aqueous media [10–12].

Phosphinic acid derivatives have also been widely employed as building units in coordination and materials chemistry [13], while carbon-supported metal adsorbents have demonstrated promising dye removal performance [14]. Recently, iron oxide-based composite nanomaterials have attracted considerable attention as efficient adsorbents for the removal of organic dyes from aqueous solutions because of their high surface area, abundant active sites, and facile magnetic separation [15–18]. Magnetite- and maghemite-containing composites combined with polymers, carbon materials, or metal oxides have demonstrated excellent adsorption capacities toward Methylene Blue and other cationic dyes [15,16]. These studies highlight the importance of developing multifunctional inorganic–organic hybrid materials with improved adsorption performance and structural stability.

The aim of this paper is to investigate the coordination behavior of the CEPPA toward Ni^{2+} and Cu^{2+} ions. Characterization techniques used for the description of Ni/Cu-CEPPA-containing systems (FT-IR, SEM, EDAX) are meant to suggest coordination through carboxylate and phosphinate oxygen atoms, morphological changes and elemental composition of the synthesized compound. The adsorption of Methylene Blue using synthesized Ni(II)/Cu(II)-CEPPA material as an adsorbent was monitored using UV-Vis spectroscopy.

2. Materials and Methods

CEPPA (2-carboxyethyl(phenyl)phosphinic acid) was achived from Carbosynth Limited (8&9 Old Station Business Park, COMPTON, Berkshire, RG20 6NE, UK). $Ni(CH_3COO)_2 \times 4H_2O$ (nickel acetate tetrahydrate), $Cu(CH_3COO)_2 \times H_2O$, and Methylene Blue were purchased from Merck (Darmstadt, Germany).

FT-IR (infrared spectroscopy) used was a PerkinElmer (Waltham, MA, USA) 100 Spectrometer with U-ATR (universal total attenuated reflectance) technique, with a frequency range of 500–4000 cm^{-1}. SEM/EDAX analyses were performed using a Quanta FEI (Hillsboro, OR, USA) 250 device.

Geometry optimizations of the CEPPA ligand and the corresponding mononuclear Ni(II)- and Cu(II)-containing complexes were performed using Density Functional Theory (DFT) as implemented in the ORCA 6.1.1 software package. The B3LYP exchange–correlation functional together with the def2-SVP basis set was employed for all calculations. TightSCF convergence criteria and RIJCOSX approximation were applied in order to improve computational efficiency.

Frontier molecular orbital (HOMO and LUMO) energies were obtained from the optimized geometries. Time-Dependent Density Functional Theory (TD-DFT) calculations were subsequently carried out using the same level of theory to investigate the electronic excitation properties of the studied systems. Ten excited states (nroots = 10) were calculated for each structure.

The resulting molecular orbitals and electronic density distributions were visualized using IQmol software (version 3.2.2).

To 20 mL solution of 2-carboxyethyl(phenyl)phosphinic acid (0.0214 g, 0.1 mmol), in distilled H_2O under continuous stirring, 0.0124 g of $Ni(CH_3COO)_2 \times 4H_2O$ (0.05 mmol) was added and the salt was left to dissolve completely for 10 min. After 10 min, 0.0121 g $Cu(CH_3COO)_2 \times H_2O$ was added and the mixture was left with continuous stirring for 30 min. The resulting mixture was transferred into a Teflon stainless-steel autoclave and heated at 180 °C for 48 h. The obtained greenish-gray solid was separated from the solution by filtration, then washed with distilled water and dried at room temperature.

3. Results and Discussion

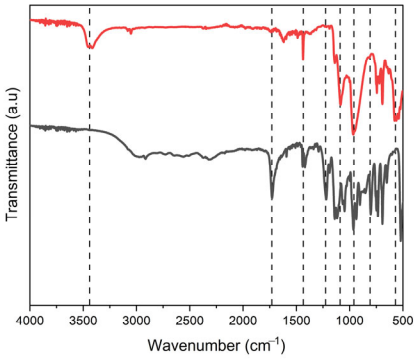
3.1. Structural Characterization

Fourier Transform Infrared Spectroscopy (FT-IR)

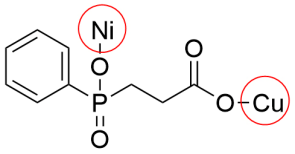
The significant differences between CEPPA and Ni/Cu-CEPPA suggest coordination of the ligand to the metal centers. A characteristic band corresponding to the carboxylic C=O group is observed at around 1702 cm^{-1} in the CEPPA. The disappearance of this band from the Ni/Cu-CEPPA, along with the asymmetric and symmetric stretching vibrations of the carboxylate group consists with the deprotonation and coordination through the carboxylate group.

A possible bidentate coordination mode is suggested by the discrepancy between σ_as(COO^-) and σ_sym(COO^-). Furthermore, discernible changes in the P–O stretching area show that phosphinate oxygen atoms are involved in coordination.

In Figure 1, a plausible coordination environment of Ni/Cu-CEPPA is proposed based on FT-IR data, consistent with coordination of phosphinate and carboxylate oxygen atoms to metal centers.



(**a**)



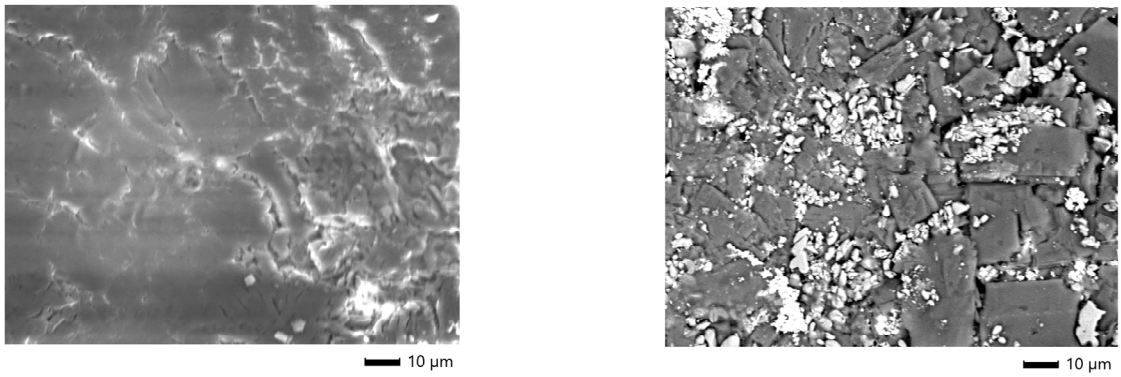
(**b**)

Figure 1. Overlapped FT-IR spectra of CEPPA (black) and Ni(II)/Cu(II)-CEPPA (red) systems (**a**); a proposed coordination environment of Ni(II)/Cu(II)-CEPPA system (**b**) (the red circles highlight the proposed coordination sites of the Ni and Cu atoms).

3.2. Morphological and Elemental Analysis

The surface morphologies of the CEPPA and Ni/Cu-CEPPA were investigated. As can be seen from Figure 2, the CEPPA (A) exhibits a relatively uniform morphology with irregularly shaped particles, while the Ni/Cu-CEPPA system (B) shows significant changes in morphology with the formation of aggregated structures and compact particles. The increased aggregation and compactness of the particles suggest the formation of a more compact aggregated morphology after metal coordination [13].

The presence of C, O, P, Ni and Cu elements (Table 1, Figure 3) in the synthesized compound is confirmed with EDAX analysis. The relative mass percentages indicate a comparable contribution of Ni (10.82%) and Cu (28.29%).



(**a**) (**b**)

Figure 2. SEM images of CEPPA (**a**) and Ni/Cu-CEPPA (**b**).

Table 1. Elemental composition of the Ni/Cu-CEPPA material determined by EDAX analysis.

Element	Mass %	Atom %
C	20.31 ± 0.25	37.64 ± 0.46
O	28.49 ± 0.33	39.65 ± 0.45
P	12.09 ± 0.17	8.69 ± 0.12
Ni	10.82 ± 0.40	4.10 ± 0.15
Cu	28.29 ± 0.77	9.91 ± 0.27

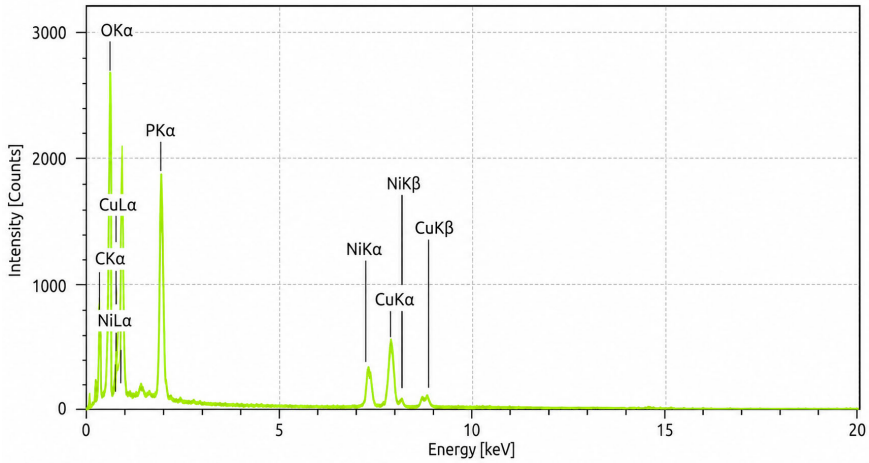


Figure 3. Representative EDX spectrum of the Ni(II)/Cu(II)-CEPPA material. The corresponding elemental composition is summarized in Table 1.

3.3. DFT Analysis of Frontier Molecular Orbitals

The Cu-containing complex exhibits a HOMO energy of −14.66 eV and a LUMO energy of −11.94 eV, with a gap of 2.72 eV, while the Ni-containing analog shows a larger HOMO–LUMO gap of 3.43 eV, with HOMO and LUMO energies of −6.36 and −2.94 eV (Table 2). The smaller ΔE value observed for the Cu complex indicates enhanced electronic reactivity and a greater tendency for charge-transfer processes, whereas the Ni complex, with a larger gap, is comparatively more electronically stable. These results suggest that the nature of the metal center significantly influences the electronic structure and reactivity of the system.

Due to the unresolved crystal structure of the mixed-metal material, DFT calculations were not intended to reproduce the exact bimetallic arrangement, but rather to provide qualitative insights into the influence of each metal center on the electronic properties.

Table 2. HOMO and LUMO energies and the corresponding energy gap (ΔE) for the Ni and Cu complexes, calculated using DFT (B3LYP/def2-SVP).

System	HOMO (eV)	LUMO (eV)	ΔE (eV)	Orbital Character
Ni-CEPPA	−6.36	−2.94	3.43	HOMO: metal-centered; LUMO: ligand-centered.
Cu-CEPPA	−14.66	−11.94	2.72	HOMO: metal/ligand contribution; LUMO: ligand-centered.

The frontier molecular orbitals (Figure 4) of both Cu and Ni complexes exhibit a metal-centered HOMO and a ligand-centered LUMO, indicating a metal-to-ligand charge-transfer (MLCT) character. The HOMO of the Ni complex shows a stronger localization on the metal center, suggesting a more pronounced d-orbital contribution, while the Cu complex displays a slightly more delocalized HOMO with increased ligand participation.

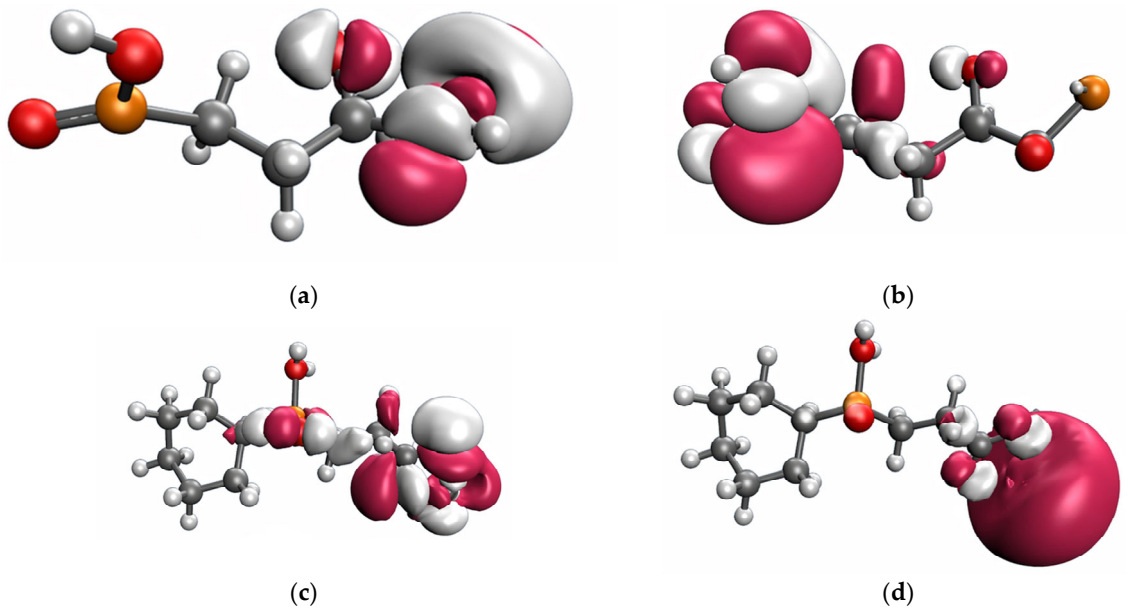


Figure 4. Frontier molecular orbitals of the Ni- and Cu-containing CEPPA complexes (calculated at the B3LYP/def2-SVP level): (**a**) HOMO-Ni; (**b**) LUMO-Ni; (**c**) HOMO-Cu and (**d**) LUMO-Cu. The red and white isosurfaces represent the positive and negative phases of the molecular orbitals, respectively.

3.4. TD-DFT Calculations

To gain insight into the electronic transitions associated with metal coordination, TD-DFT calculations were performed on the free ligand and its mononuclear Ni(II) and Cu(II) complexes. The TD-DFT results for free CEPPA show electronic transitions mainly in the deep-UV region, with the strongest calculated absorptions below 180 nm. These transitions can be assigned mainly to ligand-centered π→π* and n→π* excitations involving the phosphinate/carboxylate groups.

TD-DFT calculations for Ni–CEPPA predict low-energy transitions in the visible–near-infrared region, with the most intense transition calculated at 851.4 nm. Compared with the free CEPPA ligand, coordination to Ni(II) strongly lowers the excitation energy, indicating metal-induced modification of the electronic structure. These transitions may be associated with ligand-field and weak charge-transfer contributions.

Cu–CEPPA shows intense calculated absorption bands in the near-UV/visible region, especially at 410.2 nm, indicating strong electronic transitions after coordination with

Cu. Compared with free CEPPA, the Cu complex exhibits a marked red shift, suggesting metal–ligand charge-transfer contribution. The results are shown in Table 3.

Table 3. Calculated UV–Vis absorption bands and oscillator strengths obtained by TD-DFT calculations.

Compound	Transition	λ (nm)	f
CEPPA	3	175.6	0.04400
	15	150.4	0.03700
	7	164.5	0.02700
	12	153.7	0.02300
	18	148.7	0.02300
Ni-CEPPA	7	851.4	0.01590
	10	481.7	0.00060
	8	680.8	0.00035
Cu-CEPPA	2	410.2	1.27100
	4	375.1	0.16510
	3	376.9	0.02260

3.5. Application

Adsorption of Methylene Blue Using Ni(II)/Cu(II)-CEPPA

The adsorption of Methylene Blue was performed using 5 mg of Ni(II)/Cu(II)-CEPPA in 100 mL of solution of 50 ppm at room temperature. The quantity of Methylene Blue adsorbed (Q_e) was calculated using Equation (1):

$$Q_e = \frac{(C_0 - C_e) \times V}{m} \text{ mg/g} \quad (1)$$

C_0—initial concentration of Methylene Blue
C_e—the final concentration of Methylene Blue
V—volume of solution
m—mass of the adsorbent (Ni(II)/Cu(II)-CEPPA)
K_D (distribution coefficient) was calculated using Equation (2):

$$KD = \frac{Q_e}{C_e} \text{ L/g} \quad (2)$$

The removal capacity of Methylene Blue (%) was calculated according to Equation (3):

$$\text{Removal capacity } (\%) = \frac{(C_0 - C_e)}{C_0} \times 100 \quad (3)$$

The adsorption parameters obtained for the Ni(II)/Cu(II)-CEPPA material are summarized in Table 4.

Table 4. Methylene Blue adsorbtion.

C_0 (mg/L)	Q_e (mg/g)	K_D (L/g)	Removal Capacity (%)
50	170.24	4.103	17.024

As can be seen in Figure 5, as the contact duration increased, the distinctive Methylene Blue absorption bands, at roughly 610 and 665 nm, progressively diminished, signifying the dye's progressive removal from solution by adsorption onto the produced material. The absorption band centered at approximately 665 nm is assigned to the $\pi \rightarrow \pi^*$ electronic transition of monomeric Methylene Blue molecules within the conjugated phenothiazine

chromophore. The weaker band at around 610 nm is attributed to dimeric or aggregated forms of Methylene Blue present in aqueous solution. Under the experimental conditions investigated, an apparent adsorption plateau was observed after approximately 10 min (Figure 5). After that time, a plateau was formed. Under the experimental conditions employed (50 mg/L Methylene Blue, 5 mg adsorbent, 100 mL solution), the adsorption capacity reached 170.24 mg/g, corresponding to a dye removal efficiency of 17.02%.

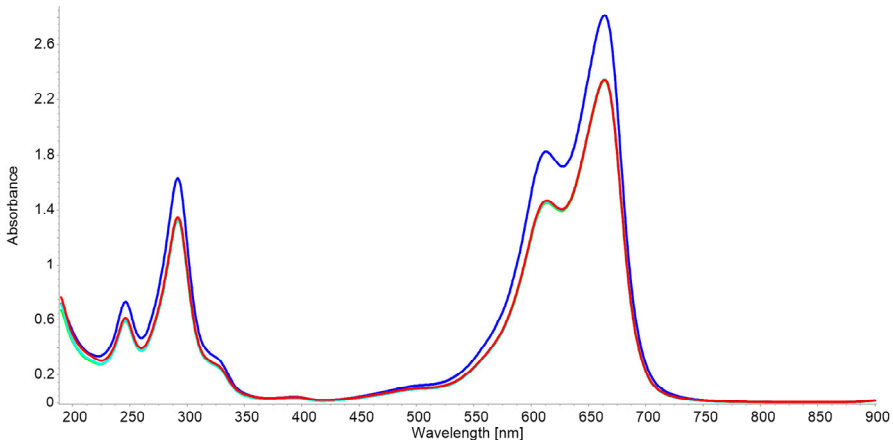


Figure 5. UV-vis absorption spectra of Methylene Blue using Cu/Ni-CEPPA as adsorbent. Methylene Blue (blue line) before adsorption and after adsorption (red line). The remaining spectra correspond to replicate measurements.

The time-dependent adsorption behavior of Methylene Blue onto the Ni/Cu-CEPPA material is presented in Figure 6.

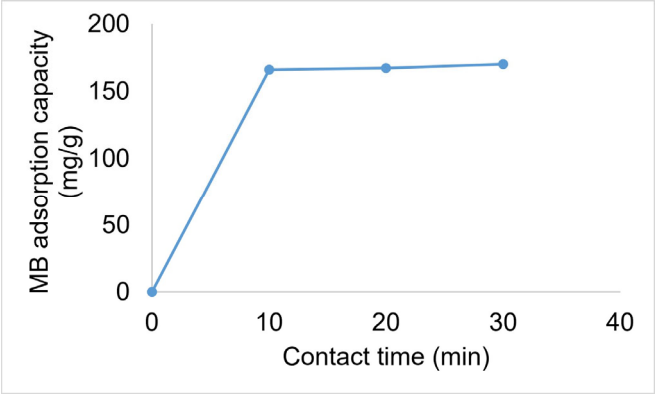


Figure 6. Time-dependent adsorption study of Methylene Blue onto the Ni/Cu-CEPPA material.

As shown in Table 5, the adsorption capacity of Ni(II)/Cu(II)-CEPPA toward Methylene Blue (170.24 mg/g) is comparable to several Cu- and Ni-containing adsorbent materials reported in the literature.

As shown in Figure 7, the adsorption capacity increased rapidly during the first 5 min and remained nearly constant from 30 to 90 min, indicating that the adsorption equilibrium was reached under the experimental conditions investigated.

The adsorption capacity (q_t) calculated from the experimental UV–Vis measurements at different contact times is presented in Table 6, according to Equation (4):

$$q_t = \frac{(C_0 - C_t) \times V}{m} \text{ mg/g} \quad (4)$$

C_t—Methylene Blue concentration at time t.

Table 5. Comparison of the Methylene Blue adsorption performance of Ni(II)/Cu(II)-CEPPA complex with recently reported materials.

Adsorbent Materials	Dye	Q_e (mg/g)	Time (min.)	Temperature (°C)	pH	Ref.
Magnetic carbon-supported metal composite	Methylene Blue (MB)	207.78	20	25	Not reported	[14]
Metal-based adsorbent system		143.3	2880	25	7	[15]
Metal-containing adsorbent composite		198.6	360	25	7	[16]
Magnetite-impregnated nanocellulose (MNC) (nanocellulose (NC) with iron oxides ($FeCl_2 \cdot 4H_2O$ and $FeCl_3 \cdot 6H_2O$) in an alkaline solution)		102.35	80	25	8	[17]
Gelatin-based functionalized carbon nanotubes@metal–organic framework (F-CNTs@MOF@Gel)		106.5	2880	25	7.9	[18]
Ni(II)/Cu(II)-CEPPA		170.24	30	25	Not reported	This work

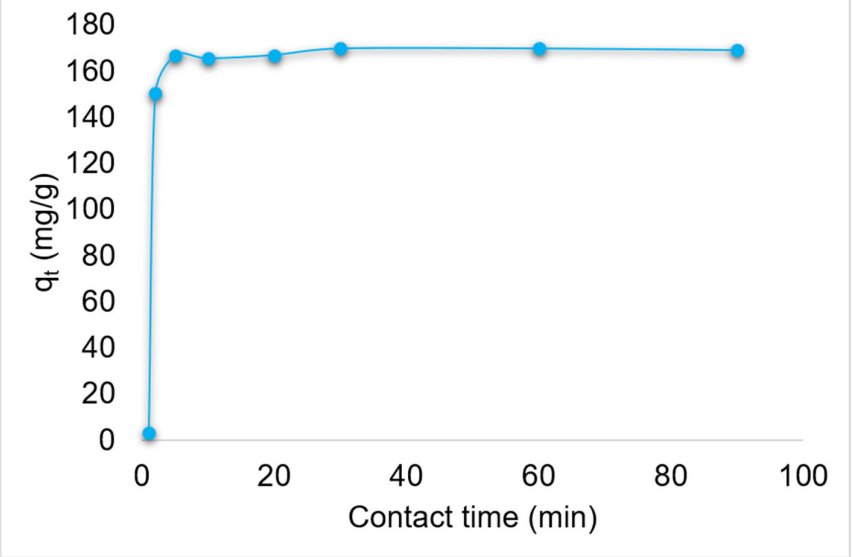


Figure 7. Effect of contact time on the adsorption capacity (q_t) of Ni(II)/Cu(II)-CEPPA toward Methylene Blue. Adsorption equilibrium was reached after approximately 30 min.

Table 6. Adsorption capacity (q_t) of Ni(II)/Cu(II)-CEPPA toward Methylene Blue as a function of contact time.

Time (min)	q_t (mg/g)
1	3.2
2	150.32
5	167.02
10	165.60
20	167.02
30	169.87
60	169.87
90	169.15

4. Conclusions

A mixed Ni(II)/Cu(II) phosphinate material based on 2-carboxyethyl(phenyl) phosphinic acid was successfully synthesized under hydrothermal conditions. FT-IR analysis suggested the coordination of the phosphinate ligand through phosphinate and carboxylate oxygen atoms, while SEM observations revealed substantial morphological changes after metal incorporation, indicating the formation of a more compact coordinated structure. The presence of both Ni and Cu was confirmed by EDAX analysis.

DFT calculations showed that the Cu-containing complex possesses a smaller HOMO–LUMO energy gap than the corresponding Ni analog, suggesting enhanced electronic reactivity and charge-transfer capability. TD-DFT calculations further demonstrated significant modifications of the electronic transitions after metal coordination, with the Cu-containing system exhibiting the most intense calculated absorption bands.

The Ni(II)/Cu(II)-CEPPA system exhibited a removal efficiency of approximately 17%. The calculated adsorption capacity reached approximately 170.24 mg/g. The combined experimental and theoretical results demonstrate that phosphinate-based mixed-metal systems may constitute potential candidates for further investigation in adsorption-related environmental applications.

It should be noted that the exact structural arrangement of the mixed-metal system could not be unequivocally established by crystallographic methods. Therefore, the coordination mode discussed herein should be regarded as a plausible model supported by spectroscopic, morphological, elemental, and computational evidence.

Further studies involving adsorption isotherms at different initial dye concentrations and detailed kinetic modeling will be performed to provide a comprehensive evaluation of the adsorption mechanism.

Author Contributions: Conceptualization, G.I. and D.A.; methodology, D.A., D.V. and V.C.; software, D.A. and D.V.; validation, G.I., D.V. and V.C.; formal analysis, D.V., V.C. and D.A.; investigation, D.V. and D.A.; resources, V.C.; data curation, D.A.; writing—original draft preparation, D.A., V.C. and D.V.; writing—review and editing, G.I., D.V., V.C. and D.A.; visualization, G.I.; supervision, G.I. and V.C. All authors have read and agreed to the published version of the manuscript.

Funding: This research received no external funding.

Data Availability Statement: The original contributions presented in this study are included in the article.

Conflicts of Interest: The authors declare no conflicts of interest.

References

1. Ahmed, M.A.; Zhernakov, M.A.; Gilyazetdinov, E.M.; Bukharov, M.S.; Islamov, D.R.; Usachev, K.S.; Klimovitskii, A.E.; Serov, N.Y.; Burilov, V.A.; Shtyrlin, V.G. Complexes of Ni(II), Co(II), Zn(II), and Cu(II): Solid-state structures and DFT calculations. *Inorganics* **2023**, *11*, 167. [CrossRef]
2. Nikolayenko, I.V.; Bazzicalupi, C.; Theron, T.-J.; Grimmer, C. Ni(II) and Cu(II) ion coordination by the novel (2*E*,2′*E*)-*N*,*N*′-(2-hydroxypropane-1,3-diyl)*bis*[(2-hydroxyimino)propanamide] ligand in the solid state and in aqueous medium. *Inorganics* **2024**, *12*, 330. [CrossRef]
3. El-Ghamry, M.A.; Elzawawi, F.M.; Aziz, A.A.A.; Nassir, K.M.; Abu-El-Wafa, S.M. New Schiff base ligand and its novel Cr (III), Mn (II), Co (II), Ni (II), Cu (II), Zn (II) complexes: Spectral investigation, biological applications, and semiconducting properties. *Sci. Rep.* **2022**, *12*, 17942. [CrossRef] [PubMed]
4. Davletshina, N.; Ermakova, E.; Dolgova, D.; Davletshin, R.; Ivshin, K.; Fedonin, A.; Stoikov, I.; Cherkasov, R. Structure and FT-IR spectroscopic analyses of complexes phosphorylated betaines with rare earth metal ions. *Inorganica Chim. Acta* **2023**, *545*, 121245. [CrossRef]
5. Pokorny, T.; Doroshenko, I.; Machac, P.; Simonikova, L.; Bittova, M.; Moravec, Z.; Karaskova, K.; Skoda, D.; Pinkas, J.; Styskalik, A. Copper Phosphinate Complexes as Molecular Precursors for Ethanol Dehydrogenation Catalysts. *Inorg. Chem.* **2023**, *62*, 19871–19886. [CrossRef] [PubMed]

6. Głowińska, A.; Trochimczuk, A.W. Polymer-Supported Phosphoric, Phosphonic and Phosphinic Acids—From Synthesis to Properties and Applications in Separation Processes. *Molecules* **2020**, *25*, 4236. [CrossRef] [PubMed]
7. Radwan, A.; Aziz, A.A.A.; Abdel-Aziz, A.M.; Sidqi, M.E.; Sayed, M.A. Harnessing synergistic effect of Al and Zn in novel bimetallic MOF for superior environmental pollutants adsorption. *Inorg. Chem. Commun.* **2025**, *179*, 114870. [CrossRef]
8. Ambrogi, E.K.; Mirica, K.A. Electronic Chemical Sensors Based on Conductive Framework Materials. *Anal. Chem.* **2025**, *97*, 4253–4274. [CrossRef] [PubMed]
9. Ahmadi, B.; Fallah, A.; Ghamarpoor, R.; Jamshidi, M. Methylene blue beyond the dye: A critical review on its role as a benchmark pollutant in photocatalyst design. *Results Chem.* **2025**, *18*, 102910. [CrossRef]
10. Oladoye, P.O.; Ajiboye, T.O.; Omotola, E.O.; Oyewola, O.J. Methylene blue dye: Toxicity and potential elimination technology from wastewater. *Results Eng.* **2022**, *16*, 100678. [CrossRef]
11. Agarwala, R.; Mulky, L. Adsorption of Dyes from Wastewater: A Comprehensive Review. *CBEN* **2023**, *10*, 326–335. [CrossRef]
12. Carhuarupay-Molleda, Y.F.; Ccasa Barboza, N.M.; Pastor-Mina, S.; Dueñas Valcarcel, C.E.; Palomino-Malpartida, Y.G.; Licapa Redolfo, R.; Mojo-Quisani, A.; Calla-Florez, M.; Aguilar-Salazar, R.F.; Flores-Ccorisapra, Y.; et al. A Study of Methylene Blue Adsorption by a Synergistic Adsorbent Algae (*Nostoc sphaericum*)/Activated Clay. *Polymers* **2025**, *17*, 2134. [CrossRef] [PubMed]
13. Kloda, M.; Ondrušová, S.; Lang, K.; Demel, J. Phosphinic acids as building units in materials chemistry. *Coord. Chem. Rev.* **2021**, *433*, 213748. [CrossRef]
14. Lv, B.; Xu, J.; Kang, H.; Liang, P.; Wang, W.; Tao, F. Adsorption behavior of magnetic carbon-supported metal nickel for the efficient dye removal from water. *Int. J. Environ. Res. Public Health* **2022**, *19*, 1682. [CrossRef] [PubMed]
15. Al-Asadi, S.T.; Mussa, Z.H.; Al-Qaim, F.F.; Kamyab, H.; Al-Saedi, H.F.S.; Deyab, I.F.; Kadhim, N.J. A comprehensive review of methylene blue dye adsorption on activated carbon from edible fruit seeds: A case study on kinetics and adsorption models. *Carbon Trends* **2025**, *20*, 100507. [CrossRef]
16. Khalaf-Allah, A.S.; Sultan, M.; Abdel-Monem, Y.K.; El-Gamasy, S.M.; El-Sayed, W.A.; Youssef, A.M. Boosting adsorption capacity of methylene blue dye by multiple functional ZnO-g-C_3N_4/carboxymethyl chitosan/alginate–grafted polyacrylic acid composite. *Sci. Rep.* **2025**, *15*, 43482. [CrossRef] [PubMed]
17. Tsade, H.K.; Melese, H.; Tadesse, A. Removal of methylene blue dye from aqueous solution using nanocellulose magnetite composites. *Water Pract. Technol.* **2026**, *21*, 1053–1067. [CrossRef]
18. Zhang, Y.; Li, Y.; Wang, M.; Chen, B.; Sun, Y.; Chen, K.; Du, Q.; Pi, X.; Wang, Y. Adsorption of methylene blue from aqueous solution using gelatin-based carboxylic acid-functionalized carbon nanotubes@ metal–organic framework composite beads. *Nanomaterials* **2022**, *12*, 2533. [CrossRef] [PubMed]

Disclaimer/Publisher's Note: The statements, opinions and data contained in all publications are solely those of the individual author(s) and contributor(s) and not of MDPI and/or the editor(s). MDPI and/or the editor(s) disclaim responsibility for any injury to people or property resulting from any ideas, methods, instructions or products referred to in the content.